1.1   THE INFRASOUND NETWORK (ISNET): BACKGROUND, DESIGN DETAILS,
AND DISPLAY CAPABILITY AS AN 88D ADJUNCT TORNADO DETECTION TOOL

A. J. Bedard, Jr.*, B. W. Bartram, A. N. Keane, D. C. Welsh, R. T. Nishiyama[1]

National Oceanic and Atmospheric Administration, Environmental Technology Laboratory, Boulder, Colorado

[1]*Cooperative Institute for Research in Environmental Sciences, University of Colorado, Boulder, Colorado*

1.   INTRODUCTION

Results from a series of field experiments indicated that detection of infrasound from tornadic storms might have potential for tornado detection and warning. A demonstration infrasonic network was designed and deployed during the spring and summer of 2003. This paper reviews the system capabilities and design elements, as well as a new "eddy fence" that permits detection of low-level infrasonic signals in the presence of high winds. A critical need was to present the acoustic data in essentially real time in forms readily interpreted and compared with radar data. The web displays developed are described using data obtained during the 2003 demonstration project.

This background paper describes infrasonic detection of tornadoes, tornadic storms, and funnels under various conditions and summarizes warning times for several case studies. The near-infrasound systems applied in this research provide a new way of "hearing" low-frequency sounds in the atmosphere and focus on a different, higher frequency window than historical infrasonic research dating to the 1970's. The purposes of this paper are to provide background for the displays provided for visualizing Infrasonic Network (ISNet) data and to describe the parameters measured.

2.   WHAT IS INFRASOUND?

Infrasound is the range of acoustic frequencies below the audible (Bedard and Georges, 2000). For a typical person, this is at frequencies below about 20 Hz, which is where the threshold of human hearing and feeling crossover. There is a rational analog between infrasound, sound and the relationship of infrared to visible light. Thus, one can call the frequency range 1 to 20 Hz near-infrasound and the range from about 0.05 to 1 Hz infrasound. Below about 0.05 Hz where gravity becomes important for propagation, atmospheric waves are usually called acoustic/gravity waves. Figure 1 indicates the sound pressure levels as a function of frequency with the threshold of human hearing as a reference.

---
* *Corresponding author address*: Alfred J. Bedard, Jr. National Oceanic and Atmospheric Administration, Environmental Technology Laboratory, Boulder, CO 80305-3328; e-mail: Alfred.J.Bedard@noaa.gov.

A frequency of 1 Hz is eight octaves below middle C. The lowest frequency on a piano keyboard is A at 27.5 Hz, consistent with being near the lowest limits of a typical person's hearing. Acousticians have adopted the convention of defining sound levels relative to the threshold of human hearing. However, infrasonic signals can be quite valuable and provide information on a range of geophysical processes. More background on infrasonics may be found at the web site http://www.etl.noaa.gov/et1/infrasound/.
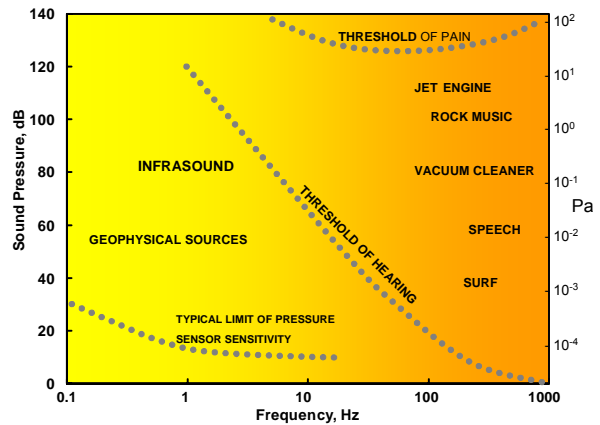
FIG. 1. Sound pressure amplitude as a function of frequency compared with the threshold of human hearing at lower frequencies. (Bedard and Georges, 2000)

3.   WHAT SENSORS AND TECHNIQUES ARE REQUIRED FOR THE DETECTION OF THESE LOW-LEVEL, LOW FREQUENCY SOUNDS?

A critical need was an effective method for reducing noise from large but highly spatially incoherent pressure fluctuations, while still detecting infrasonic signals. Daniels (1959) made the critical breakthrough with the development of a noise reducing line microphone. His concept was to match the impedance along a pneumatic transmission line using distributed input ports and pipe size changes to minimize attenuation. This innovation exploited the high spatial coherence of infrasound and the small spatial coherence of pressure changes related to turbulence, and provided signal-to-noise ratio improvements on the order of 20 dB. Variations of his concept are currently in use worldwide. Figure 2 is a photo of a spatial filter using twelve radial arms with ports at one-foot intervals and covering a diameter of fifty feet. We have adapted porous irrigation hose for

use as a distributed pressure signal transmission line (an infrasonic noise reducer), saving considerable costs in fabrication and maintenance. The present wind noise reducers can look a lot like an octopus (with four extra arms) with black porous hoses radiating outward from a central sensor.
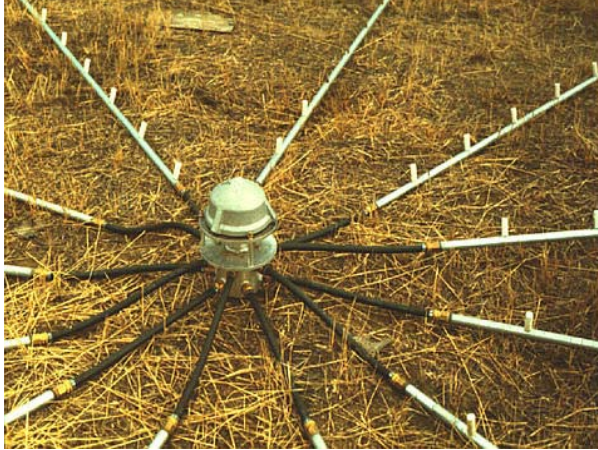
FIG. 2. Photograph of a spatial filter for reducing wind-induced pressure fluctuations in the infrasonic frequency range.

In addition, the development of an "eddy fence" (Figure 3) provides essentially all-weather detection capability. For example, we estimate that in the presence of winds of 30 ms^{-1}, signals from distant (>200 km range) tornadic storms will be detectable. The fence raises the atmospheric boundary layer and the corrugations at the top break up the wind shear layer into small, random eddies.

FIG. 3. Photograph of the 50 foot diameter eddy fence. The lower portion covered with a porous green fencing material is 6 feet high.

A reasonable assumption, for sound waves from point sources after traveling paths of tens or hundreds of wavelengths, is that the wave fronts are planar. This model is usually used in processing data from infrasonic observing systems and was the basis for the design of beam steering algorithms developed to determine correlation coefficient, azimuth, and horizontal phase speed. Effective separations for microphones in arrays are usually about one-fourth of the primary acoustic wavelength to be detected. In addition, the fact that infrasonic signals show little change with distance is the basis of the method for the reduction of unwanted pressure noise. Figure 4 shows a typical array layout. Usually, an infrasonic observatory consists of four sensors equipped with spatial filters in a roughly square configuration. The twelve porous hoses are often 50-feet in length and bent back toward the center so that the complete filter covers a diameter of about 50 feet. These noise reducers can operate in rain and snow without affecting infrasonic signals. Vegetation can reduce wind in the lower boundary layer and further improve wind noise reduction.

Array Geometry

40 to 80 meter typical spacings
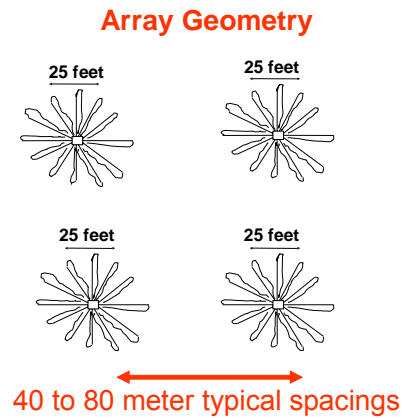
Fig. 4. View of a typical infrasonic observatory array configuration. The exact positioning of the twelve porous irrigation hoses radiating outward from each of the four sensors is not critical.

Conventional audio microphones do not respond to infrasonic frequencies. In addition to the fact that there was no practical need to detect inaudible sounds, extended low frequency sensitivity could cause undesirable dynamic response limitations. Thus, a microphone having a diaphragm deflecting in response to sound waves typically has a leakage path to a reference volume behind the membrane. This permits frequencies below the cutoff of such a high pass filter to appear on both sides of the sensor, canceling response.

We use sensitive differential pressure sensors integrated with a large, well-defined reference volume and calibrated flow resistor providing a stable high-pass filter time constant. The volume is insulated to create a stable temperature environment. These sensors are rugged, relatively small (less than 2×2×2 feet), and relatively light (about 22 pounds). They typically operate for years with few problems. Because arrays of sensors are applied to detect and process signals, there is a need to match all of the microphone sensitivities and phase characteristics. This required the creation of a family of static and dynamic pressure calibration techniques, as well as methods for measuring flow resistance. The infrasonic sensors are carefully matched and interchangeable. Table 1 summarizes the parameters measured by infrasonic observing systems.

Parameter	Significance
Correlation coefficient, a measure of signal-to-noise ratio (S/N)	Index of signal quality and a measure of confidence in the accuracy of other parameters
Azimuth	Critical measure of the direction from which sound is originating
Phase speed (Indicating the elevation angle)	Angle-of-arrival can indicate the location of source regions aloft
Spectral content	The dominant frequency (frequencies) can indicate important characteristics of the sources
Sound pressure level	The amplitude, although a measure of source strength, is greatly affected by propagation
Duration	Typical vortex-related signals continue for tens of minutes or more. Signals of very short durations (e.g. ~one minute) are unlikely to be related to a coherent vortex
Persistence	Even at low S/Ns, confidence can be obtained in the characterization of signal sources if they persist for significant periods of time. Histograms of parameters over intervals can quantify distributions and, for example, identify source direction even for weak signals

TABLE 1. Parameters measured by infrasonic observatories and their significance.

4. AT WHAT DISTANCES FROM A SOURCE CAN INFRASOUND BE DETECTED?

Cook (1962) has shown how unimportant molecular attenuation is to infrasonic propagation (5×10^{-8} dB/km), whereas sound at 2 kHz will attenuate at 5 dB/km. Since infrasound below 1 Hz is virtually unattenuated by atmospheric absorption, it is detectable at distances of thousands of kilometers from the source. Thus, an infrasonic wave at a frequency lower than 1 Hz will travel for thousands of kilometers with less attenuation than a sound wave at 2 kHz traveling for a thousand feet. Temperature changes in the atmosphere affect infrasound in the same way that light waves are refracted by lenses. In addition, wind speed changes contribute to sound refraction, guiding sound waves as they travel for long distances. Some waves escape and travel upwards to great heights in the ionosphere where they dissipate, while other sound rays are trapped and bounce back and forth many times between the earth's surface and the upper atmosphere as they travel horizontally. The atmosphere acts as a waveguide trapping much of the acoustic energy (Georges and Beasley 1977).

5. HASN'T THE USE OF INFRASOUND FOR MONITORING SEVERE WEATHER BEEN RESEARCHED SINCE THE 1970'S WITH NO OPERATIONAL USES RESULTING?

Most past observations that used acoustic passbands were much lower in frequency than the 0.5 to 5 Hz frequency range currently focused on here. This older research resulted in no operational uses for monitoring severe weather. There are significant differences between the infrasonic measurement systems applied in the 1970's and 1980's as a part of a global observing network and the higher frequency near-infrasound systems now in use. Several features of the global observing system (including the array dimensions, the spatial filter, and the sensor itself) combined to limit the high frequency response to below 0.5 Hz. The severe weather-related infrasound reported in the literature from the historic global infrasonic network involves sound two orders in magnitude longer in wavelength (λ) than the newer system and at continental scales of thousands of kilometers (e.g. Bowman and Bedard, 1971, Georges and Greene, 1975). In contrast, the near-infrasound system used to take the current measurements outlined here focuses on frequencies in the range 0.5 to 10 Hz and regional range scales of hundreds of kilometers or less. Table 2 summarizes the differences between these systems. In addition, the processes producing infrasound at extremely low frequencies are certainly quite different that those directly related to tornadoes.

System	Typical Sensor Spacing	Spatial Filter Type	Typical Acoustic λ	Max. HF Response
Historical Global Infrasound Observing System	10 km	1000 linear ft	3-30 km	0.5 Hz
Current Near-Infrasound Observing System	<100 m	50 ft in diameter	30-300 m	>20 Hz

TABLE 2. Contrasting properties of the infrasound global network and current near-infrasound observing systems.

6. HOW CAN VORTICES GENERATE SOUND?

There are a number of possible ways tornadoes and other vortices can generate sound. The conceptual view shown in Figure 5 indicates some possibilities, including shear instabilities, boundary layer sound, fluid instabilities (e.g. core bursting), and the radial modes of vibration of the vortex core.
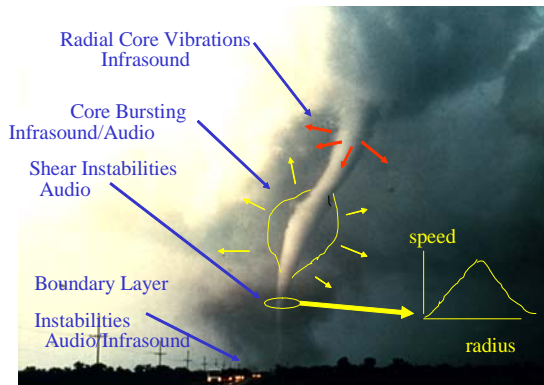
FIG. 5. Conceptual view of vortex sound generation mechanisms. Base photo of the Union City tornado (24 May 1973) after Golden.

Bedard (2002) contrasts some of these possibilities with measurements associated with tornadoes, finding that the radial vibration model (Abdullah, 1966) is most consistent with the infrasonic data. This model predicts that the fundamental frequency of radial vibration will be inversely proportional to the core radius. A radius of about 200 m will produce a frequency of 1 Hz.

7. CASE STUDIES OF INFRASOUND ASSOCIATED WITH TORNADOES AND TORNADIC STORMS

7.1 6 July 2000

At 0100 UTC on 6 July 2000, WSR-88D imagery showed an echo in southwest Nebraska moving to the south-southeast. Infrasound measured at the BAO increased abruptly from a NNE direction at about 0140 UTC and continued at high signal-to-noise ratios until about 0320 UTC. Sporadic acoustic signals continued until after 0400 UTC. The tornado hit near Dailey, Colorado at 0310 UTC, 1 hour and 30 minutes after the first infrasonic signal detection causing two injuries and 0.75 million dollars in damage. Figure 6 shows the large increase in correlation coefficient associated with this tornadic storm and Figure 7 shows the progressive azimuth shift that occurred.

As indicated in Section 5, infrasonic systems developed by the Environmental Technology Laboratory and operating at higher frequencies (above 0.5 Hz) than historical systems have provided a new view of severe weather acoustics. This has led
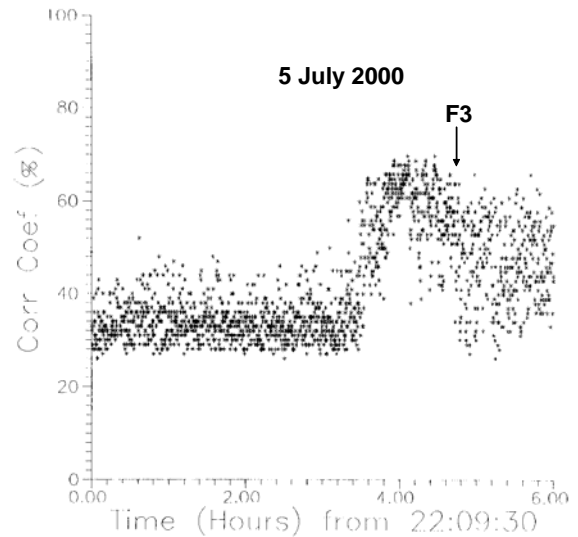
FIG. 6. Plot of correlation coefficient as a function of time for a six-hour period starting at 2209:30 UTC. The time of the F3 tornado report is indicated on the plot by an arrow.
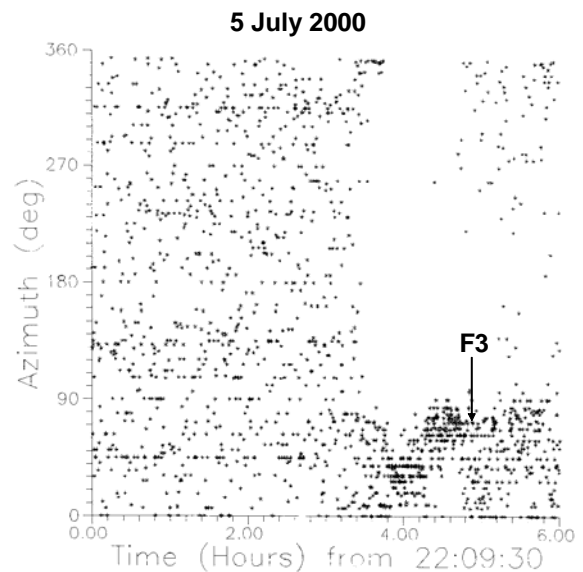
FIG. 7. Plot of azimuth as a function of time for a six-hour period starting at 2209:30 UTC. The time of the F3 tornado report is indicated on the plot by an arrow. The point of the arrow indicated the azimuth to Dailey, Colorado.

to evidence that infrasonic observatories can help address NWS goals to improve tornado warning lead times. In this section, we review a series of case study observations of low frequency sounds from tornadic storms, highlighting a number of detection scenarios and potential warning times. The evidence is that long-lived, concentrated vortices may be a common feature of some tornado producing storm types, and their detection may serve as a basis for improving warnings. A series of papers submitted to journals and in progress discusses the details of these and other cases.

7.2 *6 June 1995 (Bedard, 2004)*

A vertically concentrated vortex aloft eventually descended to the surface. Sound was detected and tracked aloft 30 minutes before the vortex reached the surface and a tornado reported. The downdraft was probably relatively weak and larger than the vortex causing downward advection but not stretching. The vortex appeared sporadically on Doppler radar until touchdown.

7.3 *31 May 1998, Spenser, SD Tornado*

A continuous vortex measured by Doppler on Wheels (Wurman, 1999) was periodically reported as a series of individual tornadoes because of variations in visibility and damage paths. After infrasound first detected the vortex (corrected for sound travel time since the distance was about 800 kilometers), the circulation produced eight tornado reports on a path over the next hour and 25 minutes. Thirty-eight minutes elapsed before a F4 tornado struck Spenser, SD. Figure 9 is a DOW image of the evolving vortex. Figure 8 shows infrasonic data, and figure 10 shows the infrasonic azimuths relative to the tornado locations.

31 August 1998

TORNADO TOUCHDOWN INTERVAL
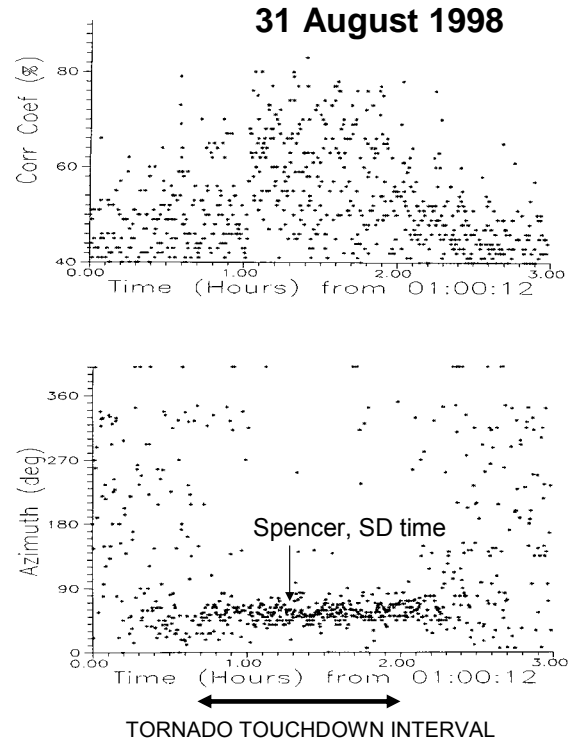
Fig. 8. Infrasound correlation coefficient and azimuth data for the BAO. The indicated tornado touchdown interval has been adjusted for acoustic travel time delay.
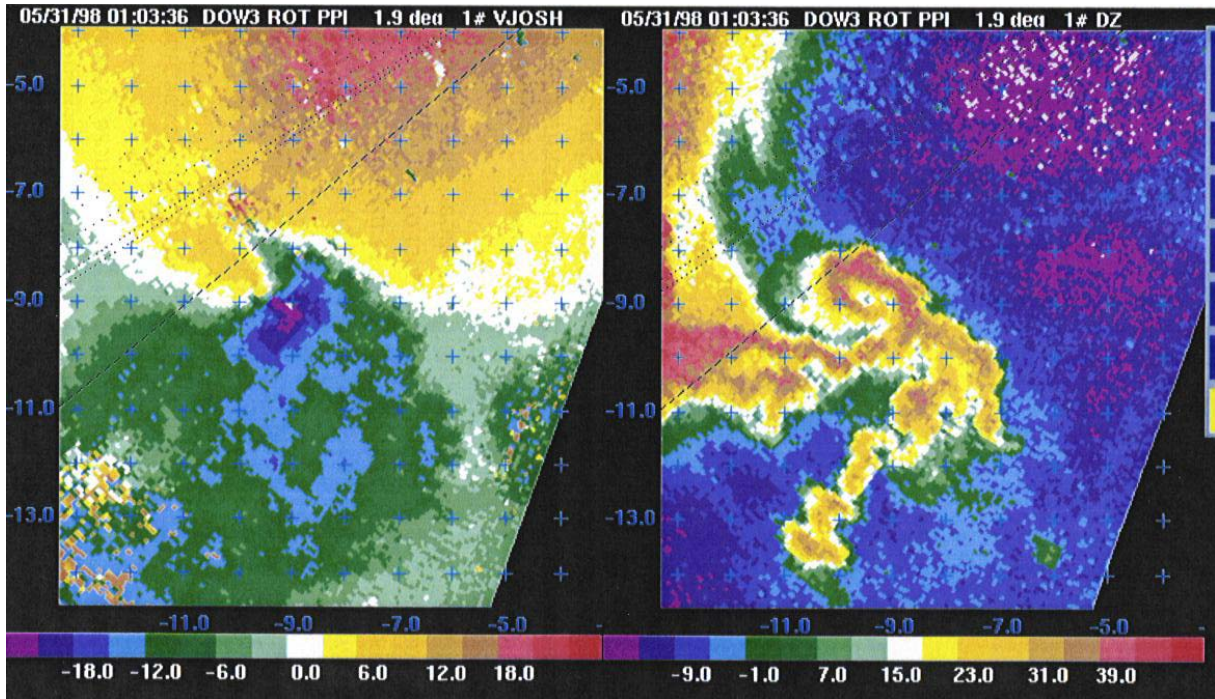
Fɪɢ. 8. Doppler radar images of radial velocity and reflectivity at 0103:36 UTC, showing the evolving tornado (with the permission of J. Wurman).

FIG. 10. Map showing the infrasonic azimuths relative to the tornado locations.

7.4 *28 June 1999 cyclic production of tornadoes*

At 0330 UTC, infrasound was first detected from the storm system. Over the next three hours, three tornadoes were reported as the system moved SSE continuously radiating infrasound. The first reported tornado was about one-hour after sound was first detected. Figure 11 is a plot of infrasonic azimuth as a function of time and clearly shows the movement of the system. The arrows indicate the times of reported tornadoes with the points of the arrows indicating the azimuth to the tornado location.

7.5 *15 June 1997*

Infrasonic signals occurred at 2111 UTC initially at high elevation angles. Ten minutes later, a tornado was reported within 3 km of the observatory in the direction from which sound was originating. The vortex was originally aloft and then probably stretched downward until reaching the surface. The photo (Figure 12) shows the tornado tapering toward the ground, where it produced a damage path 50 yards wide. Figure 13 is a map showing the position of the tornado relative to the BAO. Figure 14 is a 3-dimensional reconstruction of the tornado core made by scanning at various elevation angles, determining the dominant frequency for each, and applying the analytical model of Abdullah (1966) to calculate the core size.
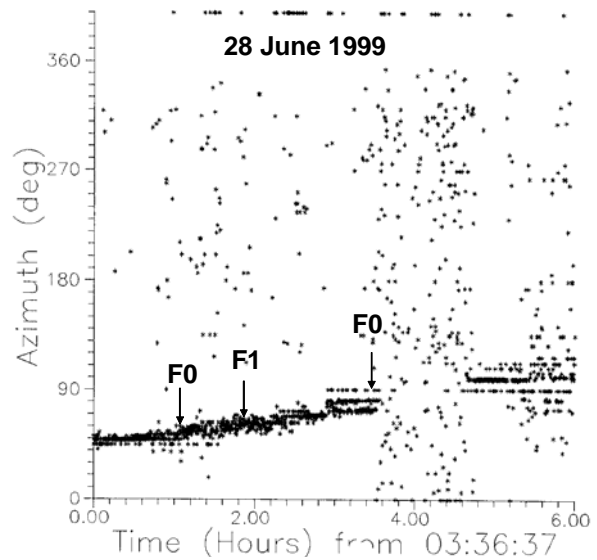
FIG. 11. Plot of azimuth of arrival of the infrasound as a function of time for a six-hour period on 28 June 1999 starting at 0336 UTC. The arrows indicate the times of tornado observations with the tips of the arrows identifying the expected azimuth of arrival.

FIG. 12. Photo of the tornado taken by police officer David Osborne and reproduced here with his permission.
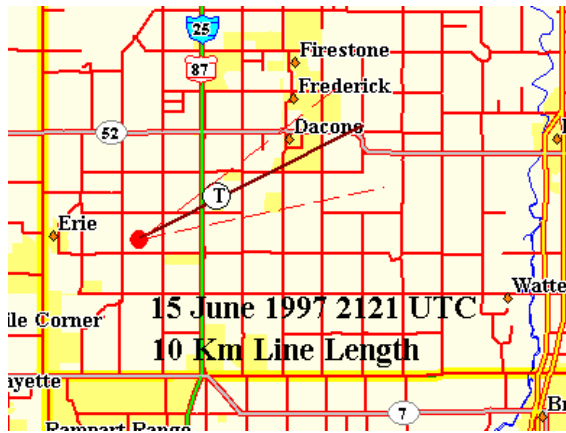
FIG. 13. Map showing the tornado location relative to the BAO.
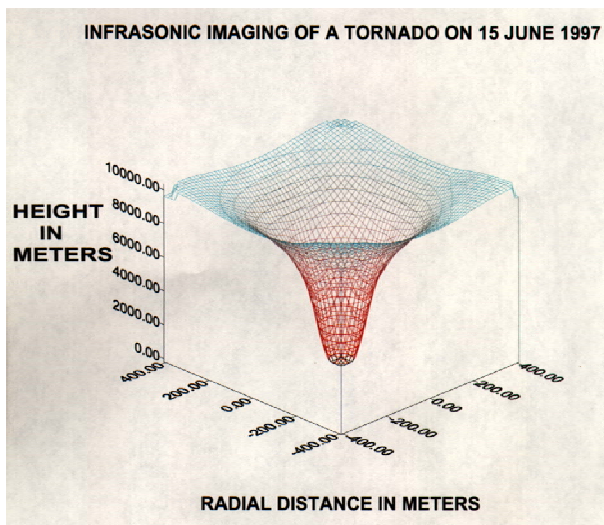
FIG. 14. A 3-D infrasonic reconstruction of the tornado core made by scanning in elevation angle and then applying the model of Abdulla (1966) to relate the dominant frequency at a series of elevation angles to estimate the vortex core size.

7.6 *"Landspout" scenario*

The production of landspouts by boundary layer vortex tilting and/or stretching is a process that can potentially occur over a fairly broad area (e.g. Szoke, 1991, Wilson, 1986, Brady and Szoke, 1989). We have detected multiple regions generating sound before and after reports of tornadoes. It is possible that only a fraction of those areas with the potential to produce tornadoes actually do so. We could possibly detect the tornado evolution processes as an updraft stretches and/or tilts the vortex. We need to obtain well-documented cases with available remote sensor data for comparison.

7.7 *Long-lived fields of short-lived funnels on 27 August 1997*

Visual observations and photographs were taken of funnels almost directly overhead while infrasound was detected from aloft. The sound occurred sporadically over a period of about one-hour, while both vertically and horizontally oriented vortices periodically appeared. These were high-based funnels (e.g. Bluestein, 1994) and did not produce tornadoes.

To place these measurements in context, we examined acoustic data for two significant large hail-producing storms studied by Doppler radar, chase teams, and aircraft. The storms showed no evidence of vortices and no infrasound occurred. This indicates that the radiation of infrasound in this frequency range is not a natural consequence of all severe weather.

The case studies summarized above indicate that infrasound is radiated by atmospheric vortices at times restricted to limited vertical heights within storms. Also, some tornadic storms produce sound continuously for durations of hours, periodically producing tornado reports. Figure 15 summarizes case study warning times. For a cyclic tornado-producing storm that is continuously radiating infrasound, we have no way to indicate when a vortex will reach the surface, but rather indicate the potential for tornado production. An assumption is that the observing site is regionally located so that acoustic delay times are not significant (<several minutes). The extent to which these cases are representative of tornado producing processes can only be evaluated with more statistics, with verified cases, and with network experience.

Vortex Downward Advection	→	**30 minutes**
Continuous Vortex[1]	→	**0 to 1 hour 25 minutes**
Cyclic Tornado Production	→	**1 to 3 hours**
Vortex Downward Stretching	→	**10 minutes**
Boundary Layer Vortex Tilting and/or Stretching	→	**Possibly 1 hour by detecting widespread processes leading to formation of landspouts**
Fields of Funnels	→	**0 to continuous monitoring**
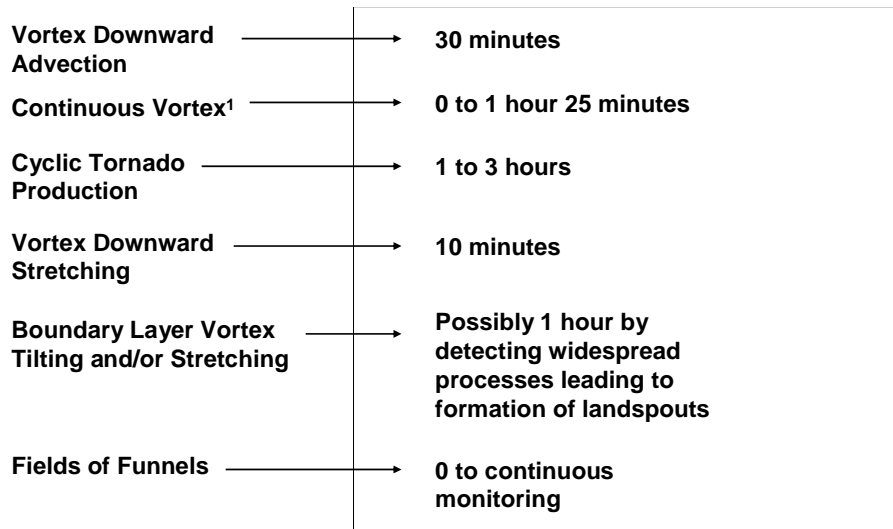
[1]A presumption is that sound was not generated until a coherent vortex had evolved

FIG. 15. Summary of case study potential warning times.

8. ARE THERE REGIONAL SIGNALS THAT CAN CAUSE FALSE ALARMS?

Typical infrasonic days in the summer (and also the spring) at the Boulder Atmospheric Observatory (BAO) east of Boulder, CO are usually free from signals that could mask severe weather signals or cause false alarms. However, we expect any regional infrasonic observatory will have a background of signals that can be systematically collected and characterized. At the BAO, there is an unusual signal that occurs almost daily during the summer months. It comes from an east northeast direction and probably originates in Nebraska. The signal usually arrives about 1500 UTC (9 a.m. MDT) and usually lasts about 15 minutes. It must involve the release of significant energy, possibly by an industrial process.

Paradoxically, such a signal (occurring outside of the strong convective time of day) can be useful as a system check or for propagation studies. In this section, this signal is used to show an example of the data visualization options under development. A survey of the infrasonic background is an effort that will help greatly with data interpretation. Strangely, shortly after the ISNet operations started in June 2003, this signal suddenly stopped appearing.

Also, we have found evidence for an association between infrasound and sprites (transient luminescent events occurring between the tops of some thunderstorms and the ionosphere) and plan a paper on this work. Indications are that this type of infrasonic signal is short and impulsive in the region of the source.
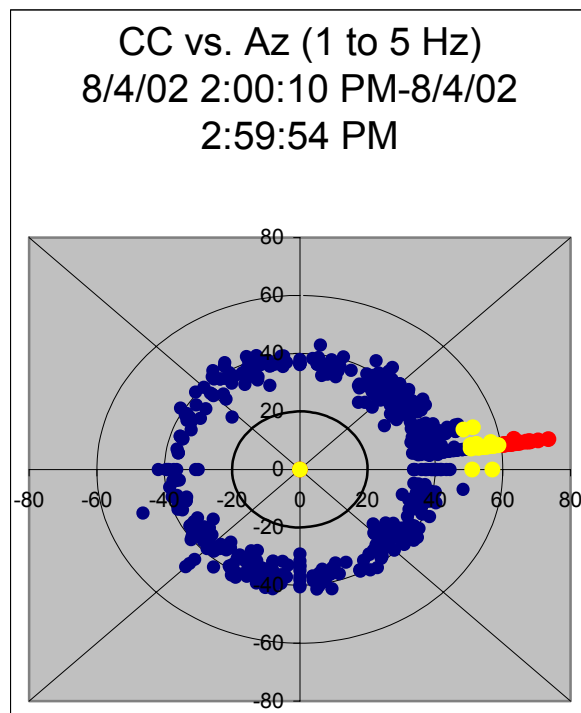
FIG. 16. Polar plot of signal azimuth data between 1400 and 1500 UTC on 4 August 2002 showing the signal from the east northeast. The data points are color coded with correlation coefficients >0.6 in red and points >0.5 yellow.
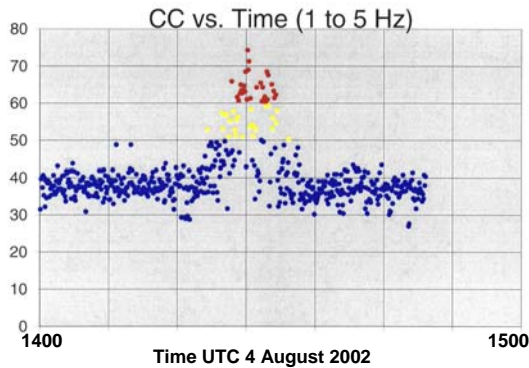
FIG. 17. Correlation coefficient as a function of time for a 1-hour interval showing the features of the recurring regional signal that is not related to severe weather. The data points are color coded with correlation coefficients >0.6 in red and points >0.5 yellow.

9. ISNET CONFIGURATION AND RATIONAL FOR LOCATION CHOICES

We took the following factors into consideration in determining the locations for the ISNet demonstration stations:

▪ Ease of logistics
The site at the BAO (Boulder Atmospheric Observatory located in Erie, Colorado) existed and the key addition was to add a data transfer link. We also benefited from assistance from the two WFO sites at Goodland, Kansas and Pueblo, Colorado.

▪ NWS offices involved
We co-located at the Goodland and Pueblo WFO's. At these two sites we were able to provide a local display which updated about every 12 seconds with new data. Data were sent to Boulder from the 3 sites over data links and presented on a web site.

▪ Locate near WSR-88D's
The WSR-88D at Goodland is on the WFO site. For the BAO and Pueblo the WSR-88D's are in the region, but not co-located.

▪ Past measurements in region
We have a long history of infrasonic measurement and testing at the BAO, where our current systems were developed. We have operated a series of field experiments in the region. This included participation in STEPS, when we installed and operated an infrasonic system at Goodland during the summer of 2000.

▪ Infrasonic environment known
We have measured the infrasonic environment in the region of eastern Colorado for over eight years with similar instrumentation and processing techniques so that the characteristics of the background of signal

types and their statistics are well-defined. Figure 18 shows a preliminary conceptual view of the ISNet stations, indicating one possible display option.

The array will make use of one existing infrasonic array at the Boulder Atmospheric Observatory, east of Boulder, Colorado. Two additional sites will be installed in conjunction with NWS radar sites in Goodland, Kansas and Pueblo, Colorado.
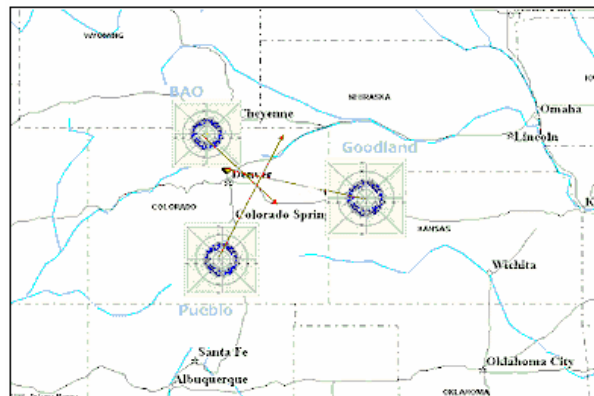
FIG. 18. Conceptual view of an early web page ISNet visualization approach. This figure shows a map of a prototype network design with the simulation of a triangulation on an infrasonic source in east central Colorado.

10. ISNET WEB SITE DISPLAYS DEVELOPED TO DATE

Figure 19 indicates the details of an ISNet station display to help interpret the visualization of infrasonic signals at a single site. Figure 20 shows a segment of a web display using real data to illustrate the options that are available.

An additional display algorithm is being tested off line. This algorithm uses the identical infrasonic data stream as described above except a histogram is created for signal azimuths from 0 to 360 degrees with a 5 degree bin size. The bin with the maximum number of points is identified and this maximum count is divided into all of the bin counts. The values multiplied by 100 are then used to create polar plots with the 40-50, 50-60, and > 60 colors described above. A key difference is that this algorithm is sensitive to lower-level but persistent signals.

Figure 21 shows the "standard" web display 0124 UTC near the time (0125 UTC) a tornado was reported in NE Colorado. The histogram display for this interval is also shown in Figure 22.
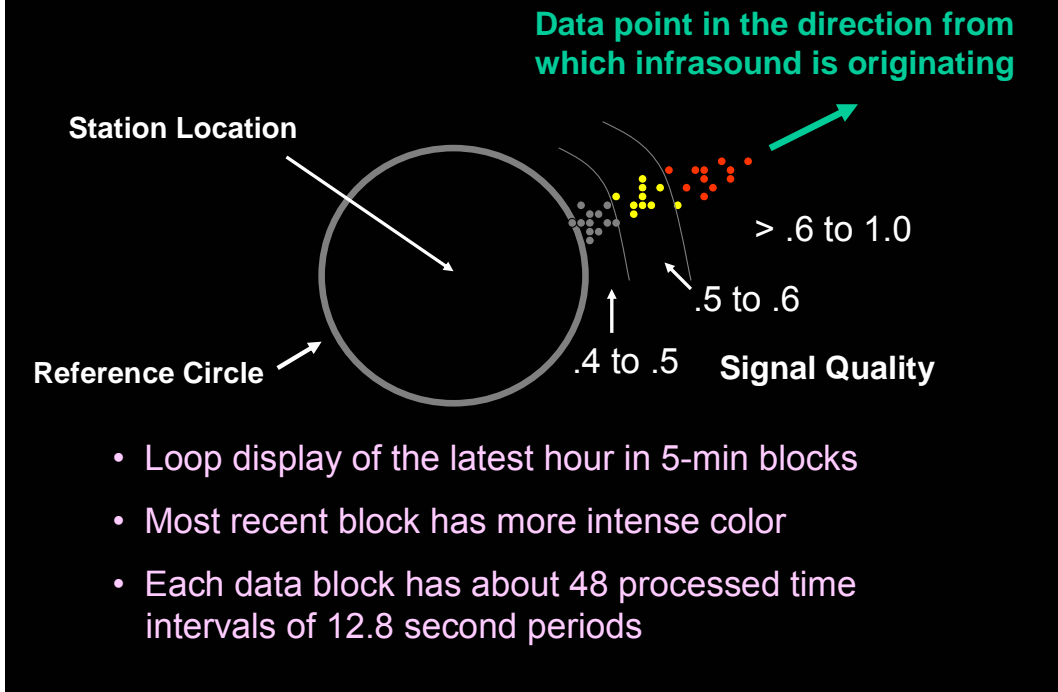
FIG. 19. Definitions of terms for interpreting infrasound signals detected at a single ISNet site.
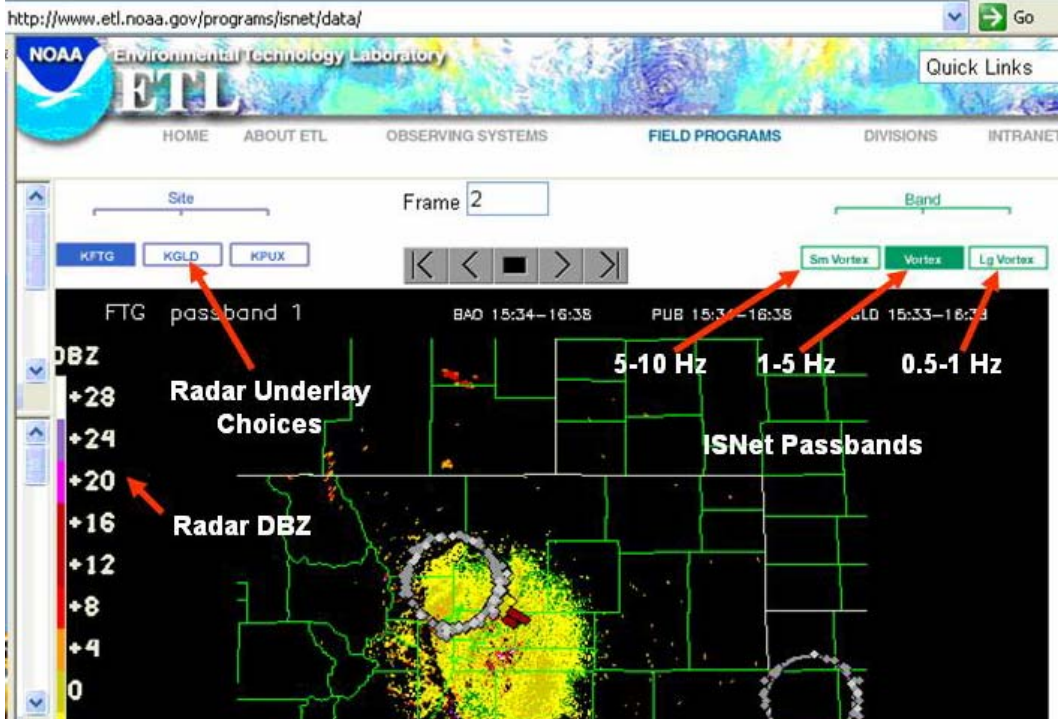
FIG. 20. An example of an actual web display showing the BAO and Goodland ISNet sites. The options for choosing radar underlays and infrasonic passbands are indicated. The 1-5 Hz passband is usually chosen for display. A signal is being detected at the BAO from the SE during this interval.
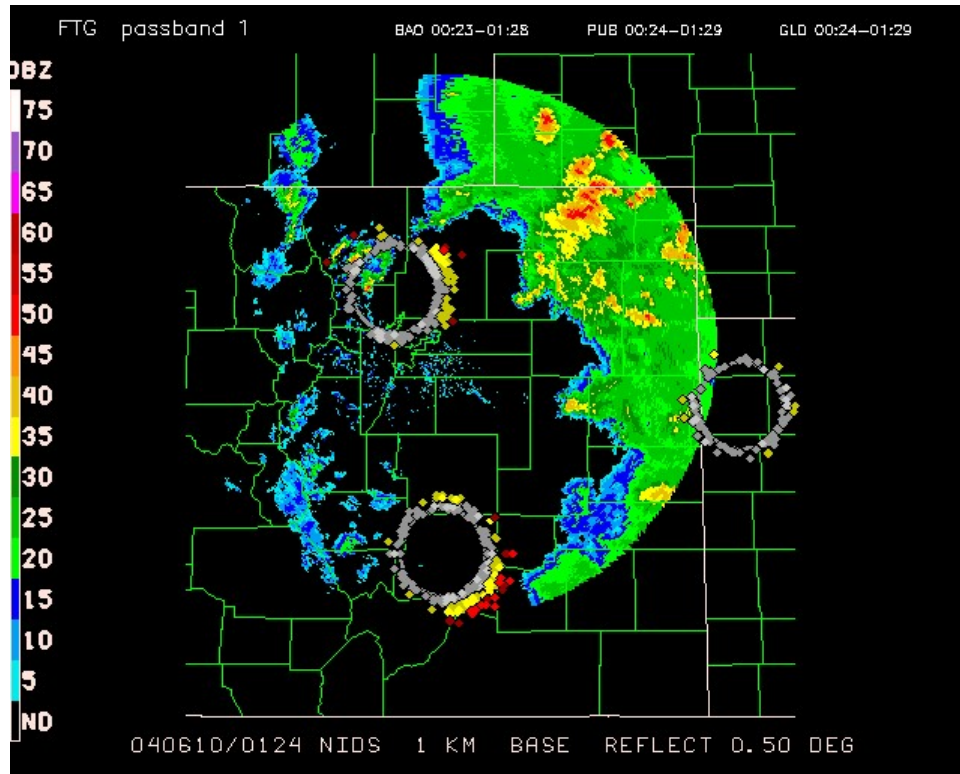
FIG. 21. Standard web display on 10 June 2004 near the time of a tornado report in NE Colorado.
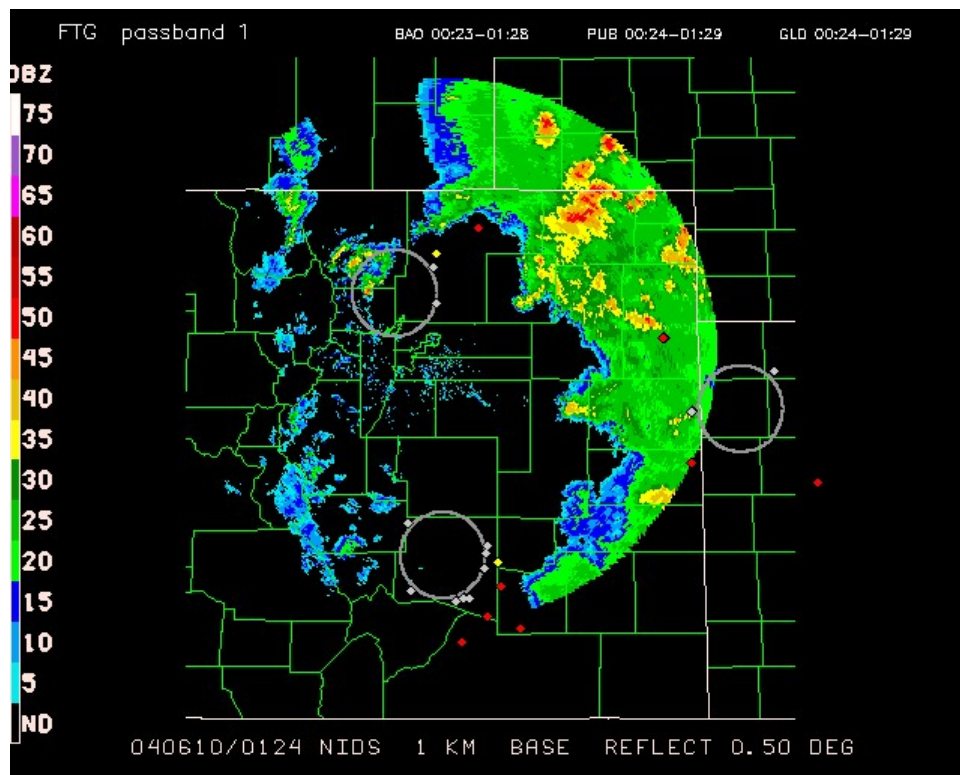
FIG. 22. Histogram experimental web display on 10 June 2004 near the time of a tornado report in NE Colorado.

Note that at this time there is a signal sector from the NE shown on the Figure 21 web display. Pueblo is detecting energy from the SE and there is little evidence of signal at Goodland. At the BAO there are gray data points from other sectors as well. In contrast, the histogram display (Figure 22) shows a sharply defined signal direction with few other directions indicated. The discrete azimuths at Goodland are from low-level noise appearing at several directions. This artifact should be able to be removed.

11. HOW CAN INFRASONIC OBSERVATORIES POTENTIALLY IMPROVE TORNADO WARNINGS?

We suggest that infrasonic observatories could possibly contribute to improving tornado warnings in the following ways:

1. Provide vortex detection capabilities where radar constraints exist (e.g. obstacle blocking, longer ranges where radar resolution is degraded, short ranges where high elevation radar scans are limited).

2. Provide detection continuity between radar scans (The interval between consecutive WSR-88D volume scans is 5 minutes).

3. Provide information on smaller diameter vortices.

4. Provide information on vortices of limited vertical extent, which may not show clearly on volume scan displays.

5. Potentially provide guidance for optimizing radar scans.

6. Provide information on vortex core size (using the sound generation model of Abdullah, 1966).

7. WHERE ARE WE NOW?

A series of papers at this conference addresses various aspects of our efforts to assess the usefulness of an infrasound network as an adjunct to the WSR-88D for tornado detection and warning. They are the following:

- **1.1**: Bedard et al. - The infrasound network (ISNet): Background, design details, and display capabilities as an 88D adjunct tornado detection tool. Oral presentation in *Technological Advances in Detection, Warnings, and Dissemination* (this paper).

- **1.2**: Szoke et al. - A comparison of ISNet data with radar data for tornadic and potentially tornadic storms in northeast Colorado. Oral presentation in *Technological Advances in Detection, Warnings, and Dissemination* (case study analysis).

- **P2.8**: Bedard et al. - Overview of the ISNet data set and conclusions and recommendations from a March 2003 workshop to review ISNet data. Poster presentation in *Hazard Mitigation, Societal Impacts, and Warnings* (provides a summary of the 2003 ISNet operations and data).

- **P2.9**: Jones et al. - Infrasonic atmospheric propagation studies using a 3-D ray trace model. Poster presentation in *Hazard Mitigation, Societal Impacts, and Warnings* (provides detailed examinations of infrasonic propagation under various atmospheric conditions, concluding that a denser network is required for robust detection under all conditions)

- **8A.3**: Nicholls et al. - Preliminary numerical simulations of infrasound generation processes by severe weather using a fully compressible numerical model. Oral presentation in *High-Resolution Numerical Modeling and Prediction of Severe Storms and Tornadoes* (numerical study of possible sound generation processes).

- **8B.8**: Hodanish - Comparison of infrasonic data and Doppler velocity data: A case study of the 10 May 2004 tornadic supercell storm over the eastern Colorado Plains. Oral presentation in *Radar and Multi-Sensor Applications* (case study analysis).

8. REFERENCES

Abdullah, A. J., 1966: The "musical" sound emitted by a tornado. *Mon. Wea. Rev.*, **6**, 213–220.

Bedard, A. J., Jr. and T. M. Georges, 2000: Atmospheric infrasound. *Physics Today*, March, 32-37.

Bedard, A. J., Jr., 2004: Low-frequency atmospheric acoustic energy associated with vortices produced by thunderstorms (accepted *Mon. Wea. Rev.*).

Bluestein, H. B., 1994: High-based funnel clouds in the southern plains. *Mon. Wea. Rev.*, **122**, 2631-2638.

Bowman, H. S., and A. J. Bedard, Jr., 1971: Observations of infrasound and subsonic disturbances related to severe weather. *Geophys. J. Roy. Astr. Soc.*, **26**, 215–242.

Brady, R. H. and E. J. Szoke, 1989: A case study of nonmesocyclone tornado development in northeast Colorado: Similarities to waterspout formation. *Mon. Wea. Rev.*, **117**, 843-856.

Cook, R. K., 1962: Strange Sounds in the Atmosphere, Part 1, *Sound*, **1**.

Daniels, F. B. 1959: Noise reducing line microphone for frequencies below 1 Hz, *J. Acoust. Soc. Amer.*, **31**, 529-531.

Georges, T. M., and G. E. Greene, 1975: Infrasound from convective storms: Part IV. Is it useful for warning? *J. Appl. Meteor.*, **14**, 1303–1316.

Georges, T. M., and W. H. Beasley, 1977: Infrasound refraction by winds. *J. Acoust.. Soc. Amer.*, **61**, 28-34.

Szoke, E. J., 1991: Eye of the Denver Cyclone. *Mon. Wea. Rev*., **119,** 1283-1292.

Wilson, J. W., 1986: Tornadogenesis by nonprecipitation induced wind shear lines. *Mon. Wea. Rev.,* **114,** 270-284.

Wurman, J., 1999: Preliminary results from the radar observations of tornadoes and thunderstorms experiment (ROTATE-98/99) *Proc. 29th International Conf. On Radar Meteorol.*, 12-16 July, Montreal, Quebec, Canada, 613-616.